Groundwater storage changes in arctic permafrost watersheds from GRACE and *in situ* measurements

2009 Environ. Res. Lett. 4 045009

(http://iopscience.iop.org/1748-9326/4/4/045009)

Environ. Res. Lett. **4** (2009) 045009 (8pp) doi:10.1088/1748-9326/4/4/045009

Groundwater storage changes in arctic permafrost watersheds from GRACE and *in situ* measurements

Reginald R Muskett and Vladimir E Romanovsky

Geophysical Institute, University of Alaska, Fairbanks, AK 99775-7240, USA

Received 7 April 2009
Accepted for publication 3 August 2009
Published 15 October 2009
Online at stacks.iop.org/ERL/4/045009

Abstract
The Arctic permafrost regions make up the largest area component of the cryosphere. Observations from the Gravity Recovery and Climate Experiment (GRACE) mission offer to provide a greater understanding of changes in water mass within permafrost regions. We investigate a GRACE monthly time series, snow water equivalent from the special scanning microwave imager (SSM/I), vegetation water content and soil moisture from the advanced microwave scanning radiometer for the Earth observation system (AMSR-E) and *in situ* discharge of the Lena, Yenisei, Ob', and Mackenzie watersheds. The GRACE water equivalent mass change responded to mass loading by snow accumulation in winter and mass unloading by runoff in spring–summer. Comparison of secular trends from GRACE to runoff suggests groundwater storage increased in the Lena and Yenisei watersheds, decreased in the Mackenzie watershed, and was unchanged in the Ob' watershed. We hypothesize that the groundwater storage changes are linked to the development of closed- and open-talik in the continuous permafrost zone and the decrease of permafrost lateral extent in the discontinuous permafrost zone of the watersheds.

Keywords: GRACE, arctic, permafrost, groundwater storage change

1. Introduction

Permafrost is the largest component of the cryosphere by area extent [1]. Degradation of ice-rich permafrost can lead to significant surface subsidence, affecting changes in the ecosystem, landscape and, where human habitats are established, causing significant infrastructure damage. The process of surface freezing and thawing, growth and degradation of permafrost affects the land surface energy and moisture fluxes (balances) which in turn impact biogeochemical cycles, climate and hydrological systems [2, 3].

Terrestrial hydrological processes in the northern latitude regions are controlled by the presence or absence of permafrost and the thickness of the active layer, the top layer of soil that thaws and freezes in the seasonal cycle [4, 5]. Beneath the active layer and within permafrost are layers and vertical bodies of unfrozen material, *talik* [6]. Talik is formed by hydrothermal and thermal processes near and beneath the ground surface [7]. Closed-talik can be laterally extensive within permafrost and beneath rivers. Meander migration on the Eagle River, Yukon, Canada, north of the Arctic Circle in the continuous permafrost zone, was responsible for a thickening of about 0.55 m yr^{-1} of talik beneath the river bed based on point-bar ages determined by tree coring [8]. Open-talik is laterally enclosed by permafrost and connects the ground surface to the unfrozen material beneath permafrost. Talik is most common in the discontinuous permafrost zone, and occurs within permafrost of the continuous and sporadic permafrost zones.

Permafrost, in particular ice-rich layers at depth, acts as an aquiclude which prevents storage and movement of groundwater [6]. Talik acts as an aquifer to allow for movement and temporary storage of groundwater. Groundwater occurs within taliks above permafrost and beneath lake beds and river channels. Within permafrost, groundwater held within talik is sustained by water flow through subsurface networks. Groundwater also occurs

beneath permafrost in earth materials above the freezing point of water. Where talik networks connect groundwater to river and stream networks on the surface, runoff can be sustained throughout the year, even in continuous permafrost zones with very harsh climate conditions.

Geographically diverse observations of permafrost temperature (∼2 m depth) have shown temporally and spatially non-uniform changes, mostly increases, over the 20th century [3]. These correlate well to surface air temperature changes on decadal timescales. Permafrost temperatures in eastern Siberia show the largest magnitude of increase of a few degrees centigrade whereas parts of western North America have lower magnitudes of permafrost temperature increase. Increasing surface air temperatures, from climate warming over the same period, often cannot fully account for increasing permafrost temperatures, suggesting that variability and secular trends in snow cover may be a contributing factor [9]. Satellite data suggest that the total area of thermokarst lakes (i.e. lakes formed by processes of permafrost degradation) in the continuous permafrost zone in Siberia increased by 12% over the last 30 years, while the number of such lakes increased by 4% [10].

We investigated the GRACE measurements of mass change in the Lena, Yenisei, Ob' and Mackenzie River watershed regions (figure 1). These rivers provide the bulk of freshwater flux to the Arctic Ocean, with as much as 45% by the Eurasian watersheds [11, 12]. This is an important factor in ocean salinity and sea ice conditions with feedbacks with the ice flux through Fram Strait–Greenland Sea and global thermohaline circulation [13–15]. Reservoir construction on the Eurasian watersheds in particular over the 20th century altered streamflow seasonality but had little effect on annual discharge [12, 16, 17]. In this investigation we seek to explore the linkages between the secular trends and variations in water equivalent mass change from GRACE and those of surface water components relative to the character of the permafrost distribution within the watersheds.

Figure 1. Northern hemisphere permafrost and watershed regions. Permafrost map derived in part from the UN Environmental Program Arctic Environmental Atlas. Digitized watershed outlines are based on data from ArcticRIMS.

2. Data and methods

Since February 2002, the joint US–German (National Aeronautics and Space Administration–Deutsches GeoForschungs Zentrum) Gravity Recovery and Climate Experiment (GRACE) has been providing datasets on the Earth's near-surface water equivalent mass changes [18–23]. Mass variations averaged over nominal monthly durations correspond mostly to water (i.e. water equivalent). The mass changes are coupled to high accuracy onboard GPS location determinations and star-tracking instruments to reference them to the International Terrestrial Reference Frame 2005. We employ the science level grids Release-04 (R4) Level-3 300 km smoothed grids. These grids have 1° × 1° longitude–latitude posting of the water equivalent mass change, on a nominal monthly basis, complete to degree and order 40 (D P Chambers 2008 personal communication[1]). Adjustments include removal of time-variable mass change effects from fluid and solid-body tides and atmosphere, and geoid. Previous studies have investigated estimates of basin-scale evapotranspiration, surface snow mass change and river discharge using GRACE coefficients up to degree and order 70 and higher [24–28]. We utilized a global grid for removal of glacial isostatic adjustment based on ICE-5G (VM2) provided by the GRACE science team [29]. Terrestrial GRACE water equivalent mass changes correspond to the climate-driven variation in land water storage if solid deformation effects are not factors [19, 30]. In their absence, estimates of water mass change are the summation of changes from soil moisture, river discharge, precipitation (including snow accumulation), vegetation water content and changes in water storage in the subsurface.

Global snow water equivalent estimates were derived from the NOAA Defense Meteorological Satellite Program by the SSM/I sensor. The data were provided by the National Snow and Ice Data Center (NSIDC). Snow water equivalent estimates in units of millimeters were derived using the horizontally polarized difference algorithm for the 19 and 37 GHz channels from daily orbit swath acquisitions [31]. Missing retrievals due to swath coverage gaps were interpolated from neighboring swaths. Nominal spatial resolution was about 69 × 43 km^2. Data were gridded in the equal-area Ease-grid projection system at 25 km × 25 km grid intervals.

Global vegetation water content and soil moisture were derived from the AMSR-E sensor and provided by NSIDC. Vegetation water content and soil moisture (skin layer, ∼1 cm thickness) estimates in units of kg m^{-2} and g cm^{-3}, respectively, were derived using the normalized polarization

[1] ftp://podaac.jpl.nasa.gov/pub/tellus/monthly_mass_grids/chambers-destripe/dpc200711/doc/GRACE-dpc200711_RL04.pdf

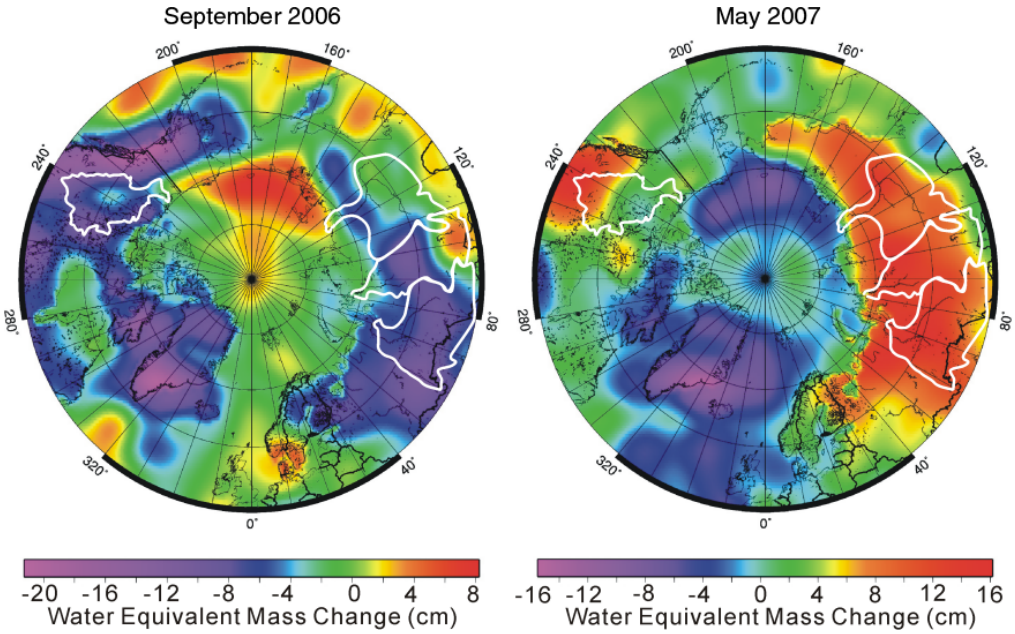

Figure 2. GRACE-derived water equivalent mass changes on the northern hemisphere during September 2006 and May 2007.

difference algorithm employing the C and X channels from global orbit swaths acquired daily [32, 33]. Nominal spatial resolution was about 38 km^2 at 10.7 GHz. Data were gridded in the equal-area Ease-grid projection system at 25 km × 25 km grid intervals. Vegetation water content derives from the leaf structure of canopy and vesicular plants on the ground.

Monthly GRACE water equivalent change, SSM/I snow water equivalent and AMSR-E vegetation water content and soil moisture were extracted within the geographic extents of the Lena, Yenisei, Ob' and Mackenzie watershed regions. Area-average sample mean, standard deviation and standard error were computed to compose time series, for the watershed total area and on 5° × 5° sub-regions. Least-squares regression was computed for each time series to derive secular trends with uncertainties.

Measurements (at gauging stations) of surface water discharge (runoff) in the watersheds were provided by ArcticRIMS (daily/monthly provisional data from 2000 to 2009) and R-Arctic-NET (archive monthly data from 1930 to 2000). Monthly discharge from stations at Kusur (Lena), Igarka (Yenisei), Salekhard (Ob') and Arctic Red River (Mackenzie) were primarily used. The archival periods of the discharged records of each watershed stations used varied in total number of years; Kusur covered a period from 1935 to 2000, Igarka from 1936 to 1999, Salekhard from 1930 to 1999, and Arctic Red River from 1972 to 2000. The archival records were compared to the provisional records to help identify discharge anomalies.

3. Results

3.1. Seasonal water equivalent mass changes

GRACE, SSM/I, AMSR-E and ground measured runoff all showed internally consistent seasonal variations within the watershed regions. GRACE minima occurred in September–October and maxima occurred in April–May. Figure 2 illustrates the GRACE water equivalent mass changes within the months of September 2006 and May 2007. These represent the seasonal minima in 2006 and maxima in 2007 on the watersheds. The timing of the minima–maxima gives rise to the shape of the time series being saw-toothed: a gradual climb in water equivalent mass during winter with a steep decline during June and afterward until minimum.

Figures 3 (Lena, Yenisei) and 4 (Ob', Mackenzie) show the monthly time series of watershed-region-averaged GRACE and SSM/I, the *in situ* mean monthly runoff (blue vertical bars) and the annual runoff time series from August 2002 through March 2008 in volume water equivalent cubic kilometers (km^3), equivalent to gigatons (Gt) of water mass changes. Annual runoff was summed from August to July over the GRACE period years; a water-year time series is traditionally from September to August. Bracketing T-bars correspond to standard deviations. SSM/I minima occurred through the late spring and summer months. SSM/I maxima occurred over February through March. The SSM/I maxima occurred ahead of the GRACE maxima by one to two months. Monthly runoff showed consistent maxima in June and minima in April. Seasonality of runoff was almost perfectly antisymmetric to GRACE seasonality. The month of the maximum in mean runoff occurred one to two months after the GRACE maxima. Note the asymmetry of the GRACE time series: the gradual increase following the minima corresponds to period of snow mass loading, and the sharp decrease following the maxima corresponds with the month of maximum runoff and water mass unloading.

SSM/I snow water equivalent had low mean values on coastal/tundra and larger mean values on interior portions of the Eurasian watersheds. The Mackenzie had low mean values of snow water equivalent on its western portions relative to

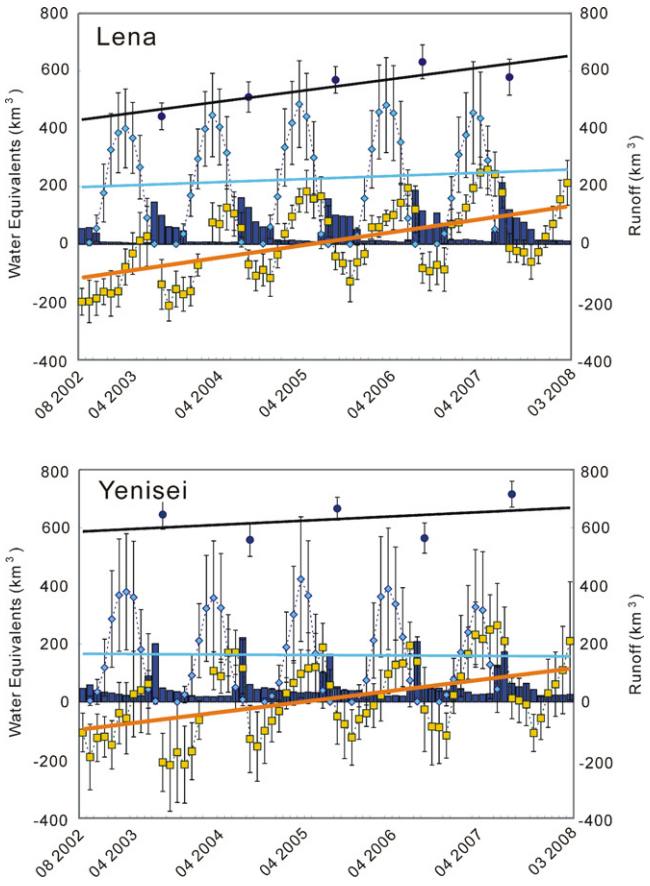

Figure 3. Water equivalent secular trends from GRACE (gold square series), SSM/I (light-blue diamond series) and runoff (monthly series as blue bar, and annual series as blue circle series) in the Lena and Yenisei River watersheds.

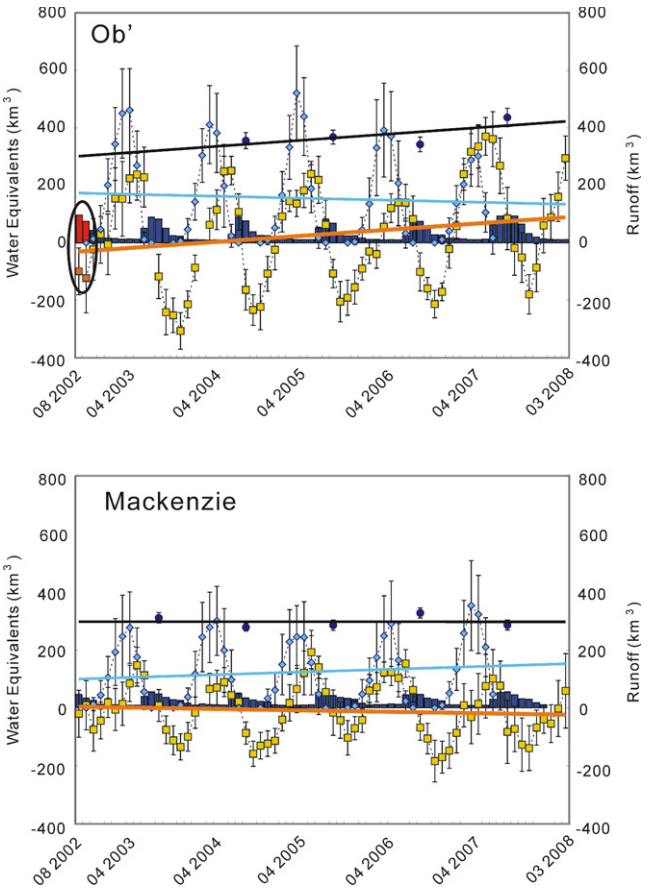

Figure 4. Water equivalent secular trends from GRACE (gold square series), SSM/I (light-blue diamond series) and runoff (monthly series as blue bar and annual series as blue circle series) in the Ob' and Mackenzie River watersheds. Two months of runoff from the Ob' are colored red with two months of GRACE circled to indicate higher water mass levels due to unseasonal (extreme) flooding events.

the eastern portions. This likely corresponds to an orographic shadow effect.

Inspection of the archival records allowed for qualitative comparison with the provisional monthly data. This analysis identified months of abnormal high runoff in August, September and October 2002 on the Ob' (figure 4, Ob' with red vertical bars). The August–September 2002 GRACE water equivalent changes (dark orange squares) reflect the additional mass from unseasonal high runoffs associated with extreme flooding in central Europe [34]. Flooding on the Ob' and other Arctic rivers has been associated with the spring snow melt, river ice break-up and precipitation [35, 36].

Monthly (daytime and nighttime) AMSR-E vegetation water content and soil moisture were averaged on the watersheds and compared to the GRACE and SSM/I time series. During winter months, AMSR-E retrievals showed very small spatially correlated vegetation water content and soil moisture values rimming large ice-covered lakes and wetlands and along the northern coasts. Skin temperatures derived from the moderate imaging spectroradiometer (MODIS) showed frozen ground conditions. We thus suspect the AMSR-E retrievals in winter to be low-limit errors of the polarization ratio retrieval algorithm. The months of December through March were then excluded from the final time series analysis. Over the period from August 2002 to March 2008, no significant increasing or decreasing trends were present. Mean vegetation water mass during April through September ranged from 5.28 ± 0.35 Gt (Mackenzie) to 7.39 ± 1.47 Gt (Ob') (table 1). Mean soil water mass over the same period ranged from 3.79 ± 0.37 Gt (Mackenzie) to 4.49 ± 0.42 Gt (Ob').

Table 1. AMSR-E mean water mass of vegetation and soil, April through September, 2002 through 2007, in the Eurasian and North American permafrost watersheds.

Watershed	Vegetation water mass	Soil water mass
Lena	6.17 ± 1.64 Gt	4.30 ± 0.31 Gt
Yenisei	7.25 ± 0.86 Gt	4.45 ± 0.46 Gt
Ob'	7.39 ± 1.47 Gt	4.49 ± 0.42 Gt
Mackenzie	5.28 ± 0.35 Gt	3.79 ± 0.37 Gt

On 5° × 5° sub-regions, latitudinal (and terrain) variations of vegetation water and soil moisture were noted. AMSR-E mean vegetation and soil water mass were lowest on the tundra (0.09 ± 0.06 Gt, 0.23 ± 0.05 Gt—Lena delta and lowlands) and higher mean values on boreal forest (0.69 ± 0.09 Gt, 0.39 ± 0.03 Gt—Yenisei uplands).

Table 2. Trends of GRACE (water equivalent mass), SSM/I (snow water equivalent) and runoff from August 2002 to March 2008 in the Eurasian and North American permafrost watersheds.

Watershed	GRACE ($km^3\ yr^{-1}$)	SSM/I ($km^3\ yr^{-1}$)	Runoff ($km^3\ yr^{-1}$)
Lena	$+44.69 \pm 8.36$	$+5.88 \pm 14.27$	$+39.35 \pm 13.30$
Yenisei	$+37.75 \pm 8.83$	-0.02 ± 9.76	$+14.64 \pm 23.22$
Ob'	$+22.69 \pm 8.49$	-0.32 ± 12.42	$+21.72 \pm 17.00$
Mackenzie	-5.58 ± 7.18	$+9.94 \pm 10.40$	-0.04 ± 7.60

3.2. Trends of water mass changes

GRACE, SSM/I and annual runoff of water equivalent mass changes in the Lena, Yenisei, Ob' and Mackenzie watersheds are given in table 2 and figures 3–5. GRACE trends indicate the Lena watershed had the largest water equivalent mass gain of 44.69 ± 8.36 $km^3\ yr^{-1}$ and the Ob' watershed had the least water equivalent mass gain of 22.69 ± 13.49 $km^3\ yr^{-1}$ of the Eurasian watersheds. The Mackenzie watershed in North America showed nominal mass loss of 5.58 ± 7.18 $km^3\ yr^{-1}$ (table 2).

SSM/I trends (table 2, figures 3–5) showed magnitudes of snow water equivalent that were one to two orders of magnitude less than GRACE trends in the Eurasian watersheds. The Mackenzie watershed trend, though of similar magnitude, was of opposite sign (increase) relative to the GRACE trend (decrease). Uncertainties in the SSM/I trends were greater than those of GRACE in the Lena, Ob' and Mackenzie watersheds, and of similar magnitude in the Yenisei watershed.

In all cases the SSM/I trends are discordant with those from GRACE (figures 3–5). This suggests snow water equivalent is not the dominant component of the increased GRACE water mass secular trends in the Eurasian watersheds. The Mackenzie watershed interestingly had a relatively strong increased trend of snow water equivalent, unlike its Eurasian counterparts. SSM/I secular trends were discordant to annual runoff trends as well.

Annual runoff trends compare well to GRACE trends in the Eurasian watersheds (table 2, figures 3–5). Uncertainties in annual runoff were much higher that those of GRACE. Runoff during August 2002 through July 2003 was not included in the Ob' annual runoff time series due to the anomalous high discharge values during August through October 2002.

4. Discussion

In our study, water equivalent mass changes from GRACE solutions up to degree and order 40 were compared with surface water changes estimated from space-borne passive microwave sensors on SSM/I and AMSR-E, and *in situ* monthly mean runoff in the Arctic permafrost watersheds of the Lena, Yenisei, Ob' and Mackenzie regions. The Lena watershed region contains an appreciable extent and volume of ground ice (Yedoma ice complex) but it and the other Siberian watersheds were not glaciated during the Pleistocene [37, 38]. Therefore, a solid Earth deformation effect on the area-averaged GRACE monthly water equivalent mass changes and secular trends can be ruled out. In the absence of signal noise and solid Earth deformation, estimates of water mass change by GRACE would be the summation of climate-driven near-surface water mass changes in the radial coordinate relative to the geoid referenced by the ITRF2005 [22]. On terrestrial watersheds and ocean basins, the relative mass changes measured in the radial coordinate (after removal of atmosphere and post-glacial rebound effects) are due to mass redistributions by pressure and gravity gradients (i.e. lateral mass transfers by *flow*).

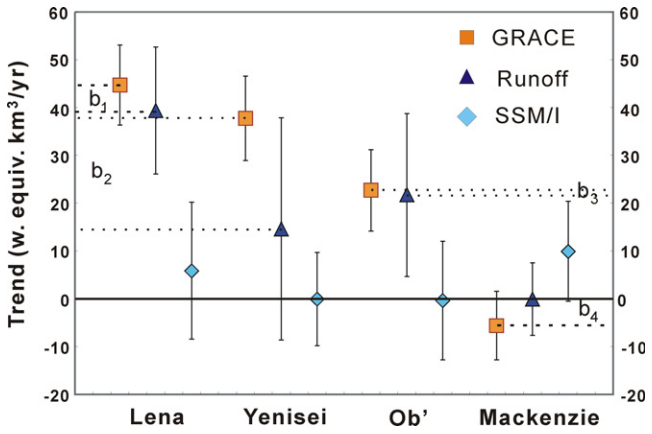

Figure 5. Comparison of secular trend magnitudes (uncertainties given by T-bar) of water equivalent changes from GRACE, runoff and SSM/I. Comparative differences of GRACE to runoff given by horizontal dashed lines and symbols (b_1 through b_4) are discussed in the text.

Examination of the time series (figures 3 and 4) indicated that GRACE water equivalent mass changes are sensitive to the timing of mass loading from winter snow water equivalent and mass unloading from spring runoff on the Arctic Eurasian and North American watersheds. Trends of water equivalent mass change showed the Lena watershed had the most water mass gain, followed by Yenisei and Ob' (figures 3 and 4 and table 2). Trends of snow water equivalent from SSM/I were near zero in the Yenisei and Ob' watersheds, and modestly increased in the Lena and Mackenzie watersheds. Annual runoff trends showed the largest increase in the Lena, followed by the Ob' and Yenisei, respectively, with the Mackenzie near zero. Qualitatively the annual runoff trends agree with trends from 1964 to 2000 [39]. For Arctic permafrost watersheds we can formulate a trend–balance relationship as

$$\Delta T_{\mathrm{GRACE}} = \Delta P + \Delta G + \Delta R. \quad (1)$$

In this formalism $\Delta T_{\mathrm{GRACE}}$ is the trend of total change observed by GRACE, ΔP is the trend of effective precipitation change (dominated by snow accumulation minus sublimation and ablation in winter and by wet precipitation minus evapotranspiration in summer), ΔG is the trend of groundwater storage change (neglecting changes in additional surface water impoundments by dams and reservoirs over the short time period) and ΔR is the trend of annual runoff from the watersheds. ΔR captures the mass of winter snow accumulation as the mass of spring snow melt.

GRACE, SSM/I and annual runoff trend magnitudes and uncertainties in the watersheds are plotted in figure 5 for

comparison. The trends of snow water equivalent from SSM/I in the Yenisei and Ob' watersheds are near zero, and those in the Lena and Mackenzie watersheds show small increases relative to GRACE and annual runoff.

Continuous permafrost, as a percentage of the total watershed area, varies from about 80% in Lena, 32% in Yenisei, 1% in Ob' and 30% in Mackenzie [40]. Given that continuous permafrost acts as an aquiclude whereas talik (unfrozen material within permafrost) acts as an aquifer, we hypothesize that the differences (b_1 through b_4, figure 5) are linked to the development of closed- and open-talik within the continuous permafrost zone, and decrease in volume occupied by permafrost in the discontinuous permafrost zone. Open-talik in continuous and discontinuous permafrost can form pathways for groundwater movement into or out of thermokarst lakes and river channels [6, 41]. Long-term expansion of existing taliks and new taliks at depth can be driven by thermokarst processes associated with river migration and lake expansion and by the more significant impact of moving groundwater on the warming of permafrost [8, 42–44]. Open-talik development and expansion could have the potential of reducing groundwater residence time by storage depletion and conversely increasing groundwater residence time by recruitment of surface water into groundwater storage. These considerations indicate equation (1) can be evaluated as

$$\Delta G \cong \Delta T_{\mathrm{GRACE}} - \Delta R \qquad (2)$$

in the Arctic permafrost watersheds of Eurasia and North America. Therefore, the differences (b_1 through b_4, figure 5) of the magnitudes of the GRACE trends with those of annual runoff trends point to three deductions.

(1) Lena and Yenisei differences suggest an increase in groundwater storage; 5.34 $\mathrm{km^3\ yr^{-1}}$ (b_1) and 23.11 $\mathrm{km^3\ yr^{-1}}$ (b_2), respectively.
(2) Ob' difference suggests nominal increase in groundwater storage; 0.98 $\mathrm{km^3\ yr^{-1}}$ (b_3).
(3) Mackenzie difference suggests a decrease in groundwater storage; 5.54 $\mathrm{km^3\ yr^{-1}}$ (b_4).

Monthly runoff of the watersheds showed increases during the seasonal minimum; Lena had $+1.22 \pm 0.38$ $\mathrm{km^3}$/April, + Yenisei had 1.29 ± 1.78 $\mathrm{km^3}$/April, Ob' had $+0.07 \pm 0.48$ $\mathrm{km^3}$/April and Mackenzie had $+0.23 \pm 0.34$ $\mathrm{km^3}$/April. The seasonal maximum on the watersheds showed increases on three and one decrease; Lena had $+15.97 \pm 3.41$ $\mathrm{km^3}$/June, Yenisei had -6.85 ± 7.75 $\mathrm{km^3}$/June, Ob' had $+0.31 \pm 1.55$ $\mathrm{km^3}$/June and Mackenzie had $+0.9 \pm 1.57$ $\mathrm{km^3}$/June. These may be due in part to water regulation practices by dams [12, 16, 17].

Permafrost and talik play a major role in drainage characteristics in Arctic watersheds [2, 45–47]. Watersheds with a low percentage of permafrost and well-developed talik have baseflow (that part of the discharge, i.e. runoff, derived from groundwater) of about 80% of discharge. Watersheds with a high percentage of permafrost and poorly developed talik have baseflow from 50% to 60% of discharge in early summer to values like those of low-permafrost watersheds. Therefore, the GRACE monthly water equivalent mass changes captured the changes of baseflow from groundwater storage changes, in addition to surface water changes in the Arctic permafrost watersheds of Eurasia and North America.

Under this interpretation we refer to figure 2, showing the GRACE-derived mass changes on the northern hemisphere in September 2006 and May 2007. Recall that those months were the respective minimum and maxima of water equivalent mass change on the Arctic watersheds. Compare these changes to those on the Chukchi and East Siberian Seas of the Arctic Ocean as illustrated (figure 2). As the Arctic watersheds were reaching their minimum in September 2006, these seas were experiencing *increased* mass, and as the watersheds were reaching their maximum in May 2007, the seas were experiencing *decreased* mass. These patterns are persistent in those months over the period from 2002 through 2007. We note that the GRACE-derived mass changes on the Arctic Ocean have multi-source barotropic and baroclinic transfers and possible spatial leakage of signal along the sea coasts [48]. Changes in freshwater discharge affect salinity, temperature and density of ocean water, which changes the mass budget and area-averaged sea level [27, 49]. A better tide model and polar motion adjustments in GRACE processing are still needed, in particular for the Arctic [50–52].

On longer timescales, significant changes of permafrost and linked responses to climate and ecosystems (water cycle and carbon stocks) have occurred [3, 4, 46, 53]. Modeling of the regional permafrost environments with general circulation model scenarios suggests significant changes in permafrost distribution are likely over the next century [5, 43, 54].

5. Conclusions

In this paper we have examined monthly water mass changes from GRACE, SSM/I, AMSR-E and station-recorded discharge of the Lena, Yensei, Ob' and Mackenzie watershed regions of Eurasia and North America. The time series covered the period from August 2002 to March 2008. Comparison of the time series showed that GRACE-derived water equivalent mass changes responded closely on a monthly basis to winter snow water mass loading (SSM/I snow water equivalent) and spring water mass unloading (runoff). AMSR-E vegetation water and soil water mass time series had no increasing or decreasing trends. Differencing the GRACE and annual runoff trends showed differences that we interpret as reflecting changes in groundwater storage.

(1) Lena and Yenisei showed increases in groundwater storage.
(2) Ob' showed a nominal increase in groundwater storage.
(3) Mackenzie showed a decrease in groundwater storage.

Whereas GRACE water equivalent mass changes on other terrestrial parts of the globe derive from surface water changes, on the permafrost watersheds GRACE captured water mass changes from changes in groundwater storage. We hypothesize that these groundwater storage changes are linked to the development of new closed- and open-talik within the continuous permafrost zone, and a decrease in volume

occupied by permafrost in the discontinuous permafrost zone. In particular, development of new open-talik in the former zone and expansion of existing open-talik in the latter could have the potential of reducing groundwater residence time by storage depletion (Mackenzie watershed) and conversely increasing it by recruitment of surface water into groundwater storage (Lena and Yenisei watersheds).

Acknowledgments

This work was funded through supporting grants from NASA (NNOG6M48G) and Alaska EPSCoR National Science Foundation award EPS-0701898 and the State of Alaska. The managers and participants in the ArcticRIMS and R-Arctic-NET services are thanked for providing provisional and archive hydrologic datasets. The Japan Aerospace Exploration Agency is thanked for use of their cluster computing facility at the International Arctic Research Center. The Alaska Region Supercomputing Center is thanked for providing computing facilities support. GRACE data were processed by Dr D P Chambers, supported by the NASA Earth Science REASoN GRACE Project (http://grace.jpl.nasa.gov). RRM performed the work for this research at the International Arctic Research Center. We thank the reviewers for constructive comments that improved the manuscript.

References

[1] Zhang T, Berry R G, Knowles R G, Heginbottom J A and Brown J 1999 Statistics and characteristics of permafrost and ground-ice distribution in the Northern hemisphere *Polar Geogr.* **23** 132–54

[2] Sergueev D O, Tipenko G S, Romanovsky V E and Romanovskii N N 2003 Evolution of mountain permafrost as a result of long-term climate change (in Russian) *Earth Cryosphere* **7** 15–22

[3] Romanovsky V E, Sazonova T S, Balohaev V T, Shender N I and Sergueev D O 2007 Past and recent changes in air and permafrost temperatures in eastern Siberia *Glob. Planet. Change* **56** 399–413

[4] White D *et al* 2007 The arctic freshwater system: changes and impacts *J. Geophys. Res.* **112** G04S54

[5] Zhang Y, Chen W and Riseborough D W 2008 Transient projections of permafrost distribution in Canada during the 21st century under scenarios of climate change *Glob. Planet. Change* **60** 443–56

[6] Woo M K 1993 *Northern Hydrology in Canada's Cold Environments* ed H M French and O Slaymarker (Montreal and Kingston CA: McGill-Queen's University Press) pp 117–42

[7] Tumel N 2002 *The Physical Geography of Northern Eurasia* ed M Shahgedanova (Oxford: Oxford Univ. Press) chapter 6 (Permafrost) pp 149–68

[8] Crampton C B 1979 Changes in permafrost distribution produced by a migrating river meander in the northern Yukon Canada *Arctic* **32** 148–51

[9] Osterkamp T E 2007 Characteristics of the recent warming of permafrost in Alaska *J. Geophys. Res.* **112** F02S02

[10] Smith S L, Burgess M M, Riseborough D and Nixon F M 2005 Recent trends from Canadian permafrost thermal monitoring network sites *Perma Perigl. Process.* **16** 19–30

[11] Aagaard K and Carmack E C 1989 The role of sea ice and other fresh waters in the Arctic circulation *J. Geophys. Res.* **94** C10 14485–98

[12] Adam J C, Haddeland I, Su F and Lettenmaier D P 2007 Simulation of reservoir influences on annual and seasonal streamflow changes for the Lena, Yenisei, and Ob' rivers *J. Geophys. Res.* **112** D24114

[13] Steele M and Boyd T 1998 Retreat of the cold halocline layer in the Arctic Ocean *J. Geophys. Res.* **103** 10419–35

[14] McDonald R W, Carmack E C, McLaughlin F A, Falkner K K and Swift J H 1999 Connections among ice, runoff and atmospheric forcing in the Beaufort Sea *Geophys. Res. Lett.* **26** 2223–6

[15] Broecker W S 1997 Thermohaline circulation, the Achilles heel of our climate system: will man-made CO_2 upset the current balance? *Science* **278** 1582–8

[16] Yang D, Kane D L, Hinzman L D, Zhang X, Zhang T and Ye H 2002 Siberian Lena River hydrologic regime and recent changes *J. Geophys. Res.* **107** 4694

[17] Yang D Q, Ye B S and Shiklomanov A 2004 Stream flow changes over Siberian Yenisei River Basin *J. Hydrol.* **296** 59–80

[18] Tapley B D, Bettadpur S, Ries J C, Thompson P F and Watkins M M 2004 GRACE measurements of mass variability in the Earth system *Science* **305** 5683

[19] Wahr J, Swenson S, Zlomicki V and Velicogna I 2004 Time-variable gravity from GRACE: first results *Geophys. Res. Lett.* **31** L11501

[20] Wahr J, Swenson S and Velicogna I 2006 Accuracy of GRACE mass estimates *Geophys. Res. Lett.* **33** L06401

[21] Chambers D 2006 Observing seasonal steric sea level variations with GRACE and satellite altimetry *J. Geophys. Res.* **111** C03010

[22] Tapley B D, Bettadpur S, Watkins M and Reigber C 2004 The gravity recovery and climate experiment: mission overview and early results *Geophys. Res. Lett.* **31** L09607

[23] Thompson P F, Bettadpur S V and Tapley B D 2004 Impact of short period, non-tidal, temporal mass variability on GRACE gravity estimates *Geophys. Res. Lett.* **31** L06619

[24] Rodell M, Famiglietti J S, Chen J, Seneviratne S I, Viterbo P, Holl S and Wilson C R 2004 Basin scale estimates of evapotranspiration using GRACE and other observations *Geophys. Res. Lett.* **31** L20504

[25] Frappart F, Ramillien G, Biancamaria S, Mognard N M and Cazenave A 2006 Evolution of high-latitude snow mass derived from the GRACE gravimetry mission (2002–2004) *Geophys. Res. Lett.* **33** L02501

[26] Niu G-Y, Seo K-W, Yang Z-L, Wilson C, Su H, Chen J and Rodell M 2007 Retrieving snow mass from GRACE terrestrial water storage change with a land surface model *Geophys. Res. Lett.* **34** L15704

[27] Ramillien G, Bouhours S, Lombard A, Cazenave A, Flechtner F and Schmidt R 2008 Land water storage contributions to sea level from GRACE geoid data over 2003–2006 *Glob. Planet. Change* **60** 381–92

[28] Peltier W R 2004 Global glacial isostasy and the surface of the ice-age earth: the ICE-5G (VM2) model and GRACE *Annu. Rev. Earth Planet. Sci.* **32** 111–49

[29] Paulson A, Zhong S and Wahr J 2007 Inference of mantle viscosity from GRACE and relative sea level data *Geophys. J. Int.* **171** 497–508

[30] Davis J L, Elósegui P, Mitrovica J X and Tamisiea M E 2004 Climate-driven deformation of the solid Earth from GRACE and GPS *Geophys. Res. Lett.* **31** L24605

[31] Chang A T C, Foster J L and Hall D K 1987 Nimbus-7 SMMR derived global snow cover parameters *Ann. Glaciol.* **9** 39–44

[32] Njoku E G, Jackson T L, Lakshmi V, Chan T and Nghiem S V 2003 Soil moisture retrieval from AMSR-E *IEEE Trans. Geosci. Remote Sens.* **41** 215–29

[33] Njoku E G and Chan S K 2006 Vegetation and surface roughness effects on AMSR-E land observations *Remote Sens. Environ.* **100** 190–9

[34] Mudelsee M, Börngen M, Tetzlaff G and Grünewald U 2003 No upward trends in the occurrence of extreme floods in central Europe *Nature* **425** 116–69

[35] Kouraev A V, Zakharova E A, Samain O, Mognard N M and Cazenave A 2004 Ob' river discharge from TOPEX/Poseidon satellite altimetry (1999–2002) *Remote Sens. Environ.* **93** 238–45

[36] Syed T H, Famiglietti J S, Zlotnicki V and Rodell M 2007 Contemporary estimates of Pan-Arctic freshwater discharge from GRACE and reanalysis *Geophys. Res. Lett.* **34** L19404

[37] Romanovskii N N, Hubberten H W, Gavrilov A V, Tumskoy V E, Tipenko G S, Grigoriev M N and Siegert C 2000 Thermokarst and Land–Ocean interaction, Leptev Sea region *Perma. Perigl. Processes* **11** 137–52

[38] Svendsen J I *et al* 2004 Late Quaternary ice sheet history of northern Eurasia *Quat. Sci. Rev.* **23** 1229–71

[39] McClelland J W, Déry S J, Peterson B J, Holmes R M and Wood E F 2006 A Pan-Arctic evaluation of changes in river discharge during the latter half of the 20th century *Geophys. Res. Lett.* **33** L06715

[40] Serreze M C, Bromwich D H, Clark M P, Etringer A J, Zhang T and Lammers R 2003 Large-scale hydor-climatology of the terrestrial Arctic drainage system *J. Geophys. Res.* **108** 8160

[41] Yoshikawa K, Romanovsky V, Hinzman L, Zheleznyak M, Romanovskii N and Buldovich S 2006 Intra-permafrost water and hydrological chronology a case study of aufeis and spring hydrology in continuous permafrost regions *EOS Trans. Am. Geophys.* Union Fall Meeting Suppl. Abstract U31B-07

[42] Yoshikawa K and Hinzman L D 2003 Shrinking thermokarst ponds and groundwater dynamics in discontinuous permafrost near council, Alaska *Perma. Perigl. Process.* **14** 151–60

[43] Shuur E A G *et al* 2008 Vulnerability of permafrost carbon to climate change: implications for global carbon cycle *Biogeoscience* **58** 701–14

[44] Oberman N 2008 Contemporary permafrost degradation of European north of Russia *Proc. 9th Int. Conf. on Permafrost (June–July 2008, Fairbanks, Alaska)* vol 2 (AK: University of Alaska Fairbanks Institute of Northern Engineering) pp 1305–10

[45] Sergueev D, Tipenko G, Romanovsky V, Romanovskii N and Kasymskaya M 2002 Impact of mountain topography and altitudinal zonation on Alpine permafrost evolution and ground water hydrology *EOS Trans. Am. Geophys. Union* Fall Meeting Suppl. Abstract B11D-03.

[46] Chapin F S III *et al* 2006 Summary and synthesis: past and future changes in the Alaskan boreal forest *Alaska's Changing Boreal Forest* ed F S Chapin III *et al* (Oxford: Oxford University Press) pp 332–8

[47] Buldovich S, Romanovskii N, Tipenko G, Sergeev D and Romanovsky V 2008 Permafrost dynamics within an upper Lena River tributary: modeled impact of infiltration on the temperature field under a plateau *Proc. 9th Int. Conf. on Permafrost (June–July Fairbanks Alaska)* vol 1 (AK: University of Alaska Fairbanks Institute of Northern Engineering) pp 211–4

[48] Dobslaw H and Thomas M 2007 Impact of river run-off on global ocean mass redistribution *Geophys. J. Int.* **168** 527–32

[49] Willis J K, Chambers D P and Nerem R S 2008 Assessing the globally averaged sea level budget on seasonal to interannual timescales *J. Geophys. Res.* **113** C06015

[50] Wünsch J 2002 Oceanic and soil moisture contributions to seasonal polar motion *J. Geodyn.* **33** 269–80

[51] Zhong M, Yan H, Wu X, Duan J and Zhu Y 2006 Non-tidal oceanic contribution to polar wobble estimated from two oceanic assimilation data sets *J. Geodyn.* **41** 147–54

[52] Seo K W, Wilson C R, Han S C and Waliser D E 2008 Gravity recovery and climate experiment (GRACE) alias error from ocean tides *J. Geophys. Res.* **113** B03405

[53] Ping C-L, Michaelson G J, Jorgenson M T, Kimble J M, Epstein H, Romanovsky V E and Walker D A 2008 High stocks of soil organic carbon in the North American Arctic region *Nat. Geosci.* **1** 615–9

[54] Sazonova T S, Romanovsky V E, Walsh J E and Sergueev D O 2004 Permafrost dynamics in the 20th and 21st centuries along the east Siberian transect *J. Geophys. Res.* **109** D01108